Spin Texture of Bi_2Se_3 Thin Films in the Quantum Tunneling Limit

Gabriel Landolt,[1,2] Steffen Schreyeck,[3] Sergey V. Eremeev,[4,5] Bartosz Slomski,[1,2] Stefan Muff,[1,2,6] Jürg Osterwalder,[1] Evgueni V. Chulkov,[5,7] Charles Gould,[3] Grzegorz Karczewski,[3,8] Karl Brunner,[3] Hartmut Buhmann,[3] Laurens W. Molenkamp,[3] and J. Hugo Dil[1,2,6]

[1]*Physik-Institut, Universität Zürich, Winterthurerstrasse 190, CH-8057 Zürich, Switzerland*
[2]*Swiss Light Source, Paul Scherrer Institut, CH-5232 Villigen, Switzerland*
[3]*Physikalisches Institut, Experimentelle Physik III, Universität Würzburg, Am Hubland, D-97074 Würzburg, Germany*
[4]*Institute of Strength Physics and Materials Science, Russian Academy of Sciences, Siberian Branch, Akademicheskiy prospekt 2/4, Tomsk, 634021 Russia*
[5]*Tomsk State University, Tomsk, 634050 Russia*
[6]*Institut de Physique de la Matière Condensée, Ecole Polytechnique Fédérale de Lausanne, CH-1015 Lausanne, Switzerland*
[7]*Donostia International Physics Center (DIPC) and CFM-MPC, Centro Mixto CSIC-UPV/EHU, Departamento de Física de Materiales, UPV/EHU, 20080 San Sebastián, Spain*
[8]*Institute of Physics, Polish Academy of Sciences, aleja Lotników 32/46, 02-668 Warsaw, Poland*

(Received 15 November 2013; published 7 February 2014)

By means of spin- and angle-resolved photoelectron spectroscopy we studied the spin structure of thin films of the topological insulator Bi_2Se_3 grown on InP(111). For thicknesses below six quintuple layers the spin-polarized metallic topological surface states interact with each other via quantum tunneling and a gap opens. Our measurements show that the resulting surface states can be described by massive Dirac cones which are split in a Rashba-like manner due to the substrate induced inversion asymmetry. The inner and the outer Rashba branches have distinct localization in the top and the bottom part of the film, whereas the band apices are delocalized throughout the entire film. Supported by *ab initio* calculations, our observations help in the understanding of the evolution of the surface states at the topological phase transition and provide the groundwork for the realization of two-dimensional spintronic devices based on topological semiconductors.

DOI: 10.1103/PhysRevLett.112.057601 PACS numbers: 79.60.Bm, 71.70.Ej, 73.20.At

$\mathbb{Z}_2$ topological insulators are materials with a band gap in the bulk and spin-polarized metallic states at the boundaries that are protected by topological properties of the bulk band structure [1–5]. Bi_2Se_3 belongs to this class of materials and was shown to feature surface states in the form of a single Dirac cone around $\bar{\Gamma}$ at the (0001) surface [6]. This compound has a layered crystal structure built up of quintuple layers (QLs) with a weak van der Waals coupling between them. When Bi_2Se_3 is reduced to a film of a few QL thickness, the topological surface states on both sides of the film overlap and a band gap opens [7]. This quasi-two-dimensional system is predicted to oscillate between a trivial and a quantum spin Hall insulator, the latter of which would host protected one-dimensional boundary states [8].

Experimentally, films of Bi_2Se_3 have been grown by molecular beam epitaxy on various substrates [7,9–13]. In addition to the gap opening, Zhang *et al.* observed by angle-resolved photoelectron spectroscopy (ARPES) measurements on Bi_2Se_3 films grown on a graphene double layer that the massive Dirac state for films with thicknesses below 6 QL appears to show a Rashba-like spin splitting [7]. It is still unclear how the topological surface states exactly emerge from these Rashba-split states at the topological phase transition.

Given the inherent difference between the chemical potential in the bulk and at the surface of such small band gap semiconductors [14], any technological application of the unique properties of topological insulators will most likely be based on such films. However, the strong coupling between the surface states on both sides of the film is expected to significantly influence their spin structure. Therefore an experimental verification of the spin structure of the surface states in the ultrathin limit is essential.

In this Letter, we present systematic spin-resolved ARPES (SARPES) measurements of the surface states of Bi_2Se_3 films on InP(111) with thicknesses ranging from 2 to 6 QL. We have found evidence of a Rashba-like spin splitting of the hybridized surface states. Our density functional theory (DFT) calculations model the observations and clarify the evolution of the dispersion and the localization of the surface states upon the transition from the two-dimensional limit to the three-dimensional topological insulator.

The films were grown by molecular beam epitaxy in a vertical CreaTec system, equipped with standard effusions cells for Se and Bi (99.9999% purity each) at a base pressure below 10^{-10} mbar. Undoped InP(111)B wafers were used as substrate, and their natural oxide layer was removed by a dip in 50% hydrofluoric acid. The substrate temperature during the growth was 300°C for all films. The fluxes of Bi and Se were constant, with a growth speed of 1 nm per minute, under Se rich conditions. The film thicknesses were determined by the growth time, which was calibrated by x-ray diffraction thickness fringes on a reference bulk film. After growth the samples were cooled *in situ* to a temperature below 15°C, and were then capped with amorphous Se to protect the films *ex situ* during transport. In the ARPES chamber the films were decapped by heating the sample to a temperature of about 120°C.

The ARPES and SARPES measurements were performed at the COPHEE end station of the surface and interface spectroscopy beam line at the Swiss Light Source [15]. The measurements were performed at a base pressure better than 4×10^{-10} mbar, both at room temperature and at 20 K. The three-dimensional spin information is obtained by means of two orthogonally oriented classical Mott detectors, each of which measures two spatial components of the photoelectron spin expectation value.

The electronic structure calculations are performed within the DFT with the generalized gradient approximation to the exchange correlation potential as implemented in VASP [16,17]. The exchange-correlation part of the potential was treated using the exchange-correlation functional of Perdew-Burke-Ernzerhof [18] within the projector-augmented wave methodology [19,20]. Relativistic effects, including spin-orbit coupling, were fully taken into account.

Figure 1(a) shows spin-integrated ARPES band maps of $Bi_2Se_3/InP(111)$ films with thicknesses ranging from 2 to 6 QL. The data are taken along the $\overline{\Gamma M}$ direction with *p*-polarized light of 20 eV photon energy, which placed the perpendicular momentum of the initial state around the Brillouin zone center. In the band map for the 5 QL film, dashed lines indicate the different bands contributing to the spectra. The Dirac cones (orange diamonds, red square) are separated by a band gap accompanied by a nonlinear dispersion around $\bar{\Gamma}$. Both the bulk conduction band (blue circles, green triangles) and the valence band are split into quantum well states (QWSs), due to the confinement of the states between the substrate band gap and the vacuum barrier. Their energy separation increases towards lower film thicknesses and the number of occupied QWS states decreases. The energy distribution curves in Fig. 1(b) at $\bar{\Gamma}$ clarify the evolution of the band dispersion with film thickness. The red (orange) arrows indicate the minima (maxima) of the massive electronlike (holelike) Dirac states, the blue and green arrows mark the conduction band QWSs.

Figures 1(c) and 1(d) show the band maps and energy distribution curves measured on the same samples at a photon energy of 50 eV. The spectral intensity of the QWSs is strongly reduced with respect to the surface states for all of the shown film thicknesses. This allows us to easily discern the spin polarization of the Dirac cones from the spin signal of the QWSs as will be discussed below. Previous studies suggest that the gap closes around 6 QL. Our measurements confirm a gap that is smaller than the experimental resolution at this thickness. The 6 QL band map was taken at a temperature of 20 K, the observed shift of the bands towards higher binding energies by

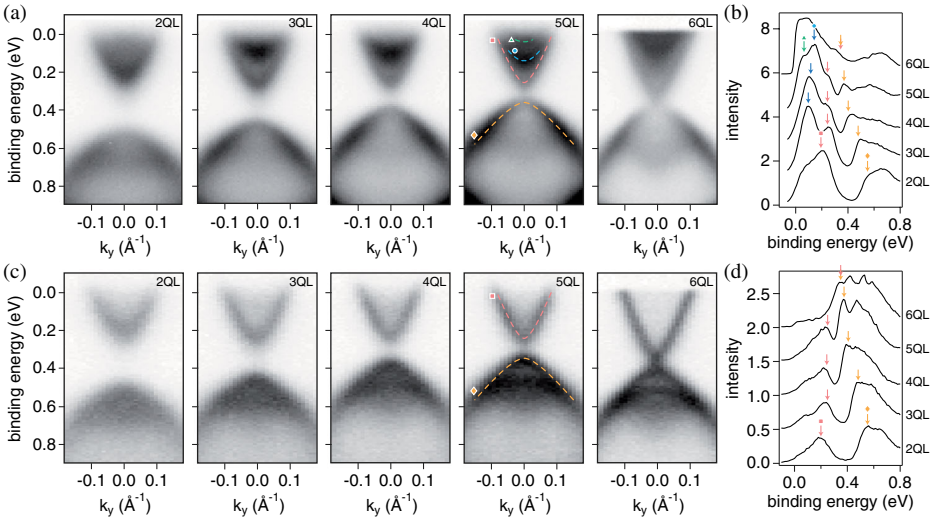

FIG. 1 (color online). (a) Band dispersion for 2–6 QL $Bi_2Se_3/InP(111)$ measured with 20 eV photon energy. (b) corresponding energy distribution curves at $\bar{\Gamma}$. (c),(d) same as (a),(b) but measured at a photon energy of 50 eV. The measurements were performed at room temperature, except for the 6 QL band map which was taken at 20 K.

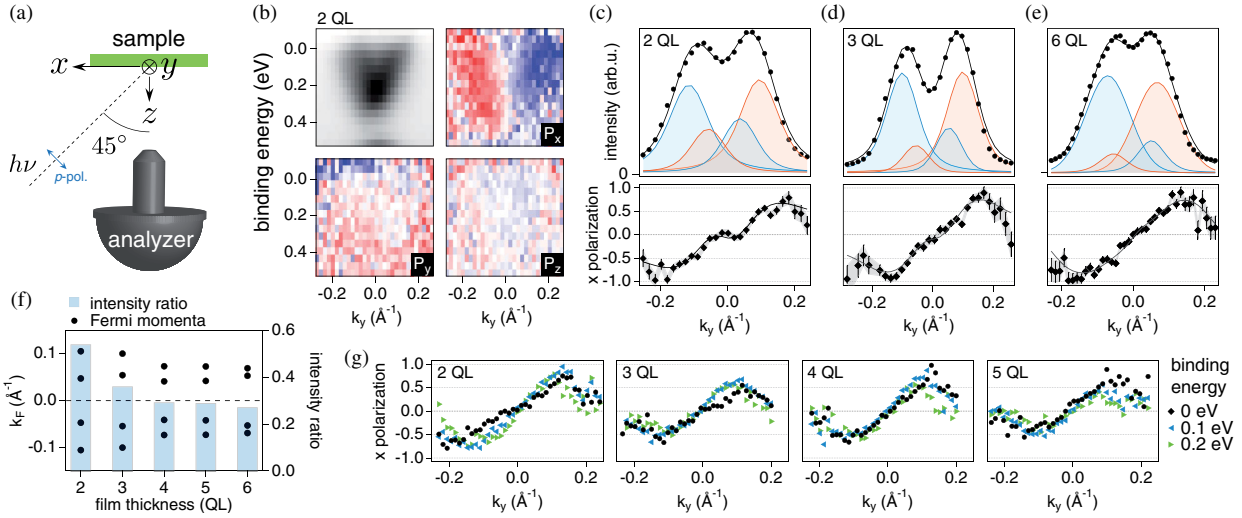

FIG. 2 (color online). (a) (S)ARPES measurement geometry. (b) Mott detector band map and spin polarization along the three spatial directions for 2 QL Bi_2Se_3/InP(111). (c) Spin-resolved momentum cut at the Fermi level for a 2 QL film, (d) 3 QL film, and (e) 6 QL film. (f) Thickness-dependent Fermi momenta obtained from fitting the spin-resolved measurements (dots) and ratio of the average intensities of the inner and the outer Rashba bands (blue bars). (g) Binding-energy-dependent x spin polarization for 2–5 QL thick films.

about 100 meV with respect to the room temperature measurements is consistently observed on all film thicknesses when measured at low temperature [21].

In Fig. 2 we present our SARPES data measured with p-polarized 50 eV photons. The measurement direction is along the y coordinate as sketched in Fig. 2(a). The orbital character of the surface states in Bi_2Se_3 films is mostly of p_z type, whereas the in-plane orbitals show a layer dependent texture [21–23]. In our measurement geometry Fermi's golden rule implies that mostly p_z and p_x orbitals are probed [23,24]. The spin-orbit interaction couples the spin of the electrons in these orbitals in a helical spin structure with the same rotation direction [22]. Therefore the measured spin polarization of the photoelectrons represents mostly the spin texture of the p_z orbitals. Systematic measurements at further photon energies and light polarizations can be found in the Supplemental Material [21].

Figure 2(b) shows the total intensity and the spin polarization components of a 2 QL film along the three spatial directions (P_x, P_y, P_z) measured with the Mott detectors at a temperature of 20 K. The spin polarization is in-plane and orthogonal to the crystal momentum (i.e., along x). The spin expectation vector circles counterclockwise on a constant energy contour, in qualitative accordance to the topological surface state of bulk Bi_2Se_3. An out-of-plane polarization is in principle allowed by the crystal symmetry for momenta along $\overline{\Gamma K}$ [25], but is not observed.

Higher statistics spin-resolved momentum distribution curves on the same 2 QL sample reveal the existence of an inner pair of bands with opposite spin polarization, as shown in Fig. 2(c). These inner bands lead to a plateau in the x polarization around the $\bar{\Gamma}$ point, as seen in the bottom panel. The upper panel shows the total Mott detectors intensity (black dots) and the individual peaks of the bands obtained by simultaneously fitting the total intensity and the spin polarization [26]. The momentum splitting at the Fermi level gradually decreases from about 0.058 $Å^{-1}$ at 2 QL to 0.016 $Å^{-1}$ at 6 QL. The intensity of the inner bands is suppressed with respect to the outer band and consequently the plateau in the vicinity of the $\bar{\Gamma}$ point is less pronounced and the peaks in the spin-resolved intensity have lower amplitudes, Figs. 2(d) and 2(e). Figure 2(f) summarizes the shrinking spin splitting and the intensity reduction of the inner bands at the Fermi level. Our spin-resolved measurements at other photon energies show an anticipated energy dependence of the absolute value of the measured spin polarization and confirm the reported spin structure [21].

Furthermore, we compare spin-resolved measurements at different binding energies for various thicknesses in Fig. 2(g). There is a small decrease of the spin signal amplitude when comparing the measurements closer to the band apex to the data taken at the Fermi level. This behavior is in principle expected due to the larger delocalization throughout the film along the out-of-plane direction for the state towards the band apex (see discussion below). Most of the observed reduction, however, must be attributed to the increasing angular overlap of the experimentally broadened bands.

At the Fermi level the Dirac states are spin polarized with an intrinsic degree of polarization that is almost independent of the film thickness also when compared to the gapless case in the bulk limit [21]. The experimentally measured polarization amplitudes do not significantly decrease towards smaller film thicknesses despite the larger spectral weight of the oppositely polarized inner branches.

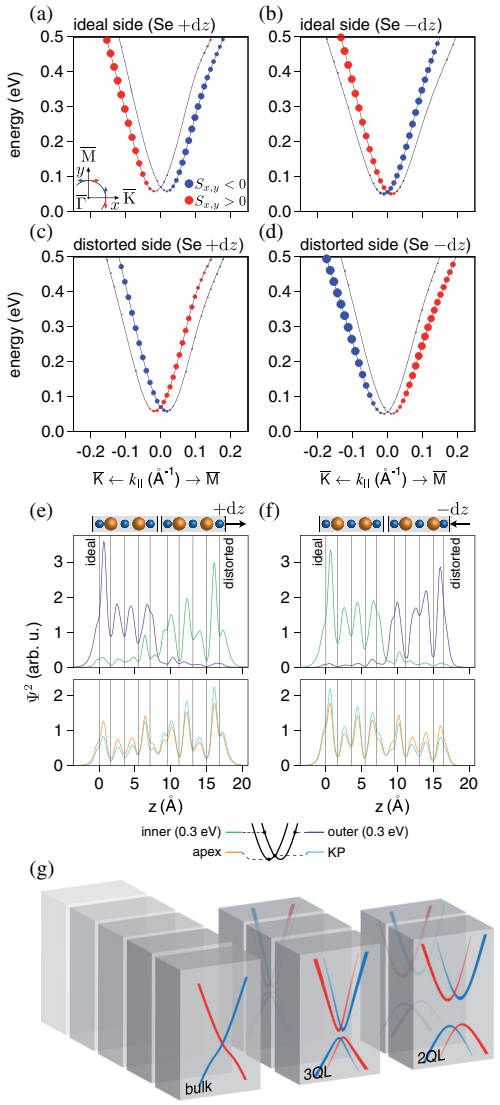

FIG. 3 (color online). DFT calculations of a freestanding 2 QL Bi_2Se_3 film where one of the Se surface layers is artificially displaced towards vacuum ($+dz$) or towards the crystal ($-dz$). (a),(b) Dispersion of the electronlike spin-split massive Dirac state (black); the size of the colored data points indicate the weight of the wave function in the ideal surface QL. (c),(d) Weight of the wave function in the QL with the displaced surface layer. (e),(f) Charge density distribution along the stacking axis z for different energies: $E = 0.3$ eV, at the Kramer's point (KP) and the band apex. (g) Schematic band evolution.

This is also in contrast to previous theoretical predictions for symmetric films [27] and shows the importance of the choice of substrate for the utilization of ultrathin topological insulators.

In order to mimic the substrate-induced symmetry breaking in our DFT calculations, the Se surface layer of the freestanding Bi_2Se_3 films is artificially displaced along the surface normal, either towards the crystal bulk ($-dz$) or towards the vacuum ($+dz$). Figure 3 shows the results for a 2 QL thick film. The spatial overlap leads to a hybridization of the two surface states and a gap opens around the Dirac point. Because of the missing structural inversion symmetry the two massive Dirac states are split in a Rashba-like manner but with distinct localization of the inner and outer branches depending on the direction of displacement of the Se surface layer. The spatial localization is indicated by the size of the colored data points, the color indicates the sign of the net spin polarization. For a $+dz$ displacement the inner (outer) branches are mainly localized at the ideal (distorted) surface as shown in Figs. 3(a) and 3(c), and vice versa for a $-dz$ displacement, Figs. 3(b) and 3(d). Towards the band apex below the Kramer's point, however, the states become delocalized throughout both QLs due to the hybridization, as shown in Figs. 3(e) and 3(f). With increasing film thickness but keeping the surface layer displacement constant, the wave function overlap and the gap diminish and the splitting decreases. Finally, the gapless topological surface states emerge.

Our measurements suggest that the effect of the InP(111) substrate is mimicked in this model by a $+dz$ displacement of the Se layer which is equivalent to a small charge transfer from the film to the substrate. The smaller spectral intensity of the inner branches and its continuous reduction towards thicker films [Fig. 2(c) and [21]] indicate that the outer (inner) branches are localized in the QL at the surface (film-substrate interface). This contrasts with the situation of Bi_2Se_3 films grown on a double layer graphene on top of a 6H-SiC substrate where the inner branches are localized at the film surface, considering the spectral intensity distribution and the evolution of dispersion with film thickness [7]. On the other hand, for Bi_2Se_3 films grown on Si(111) no such splitting could be resolved up to now [10]. These observations are in line with other Rashba systems where the splitting is known to be determined by the relative spatial shift of the wave function with respect to the atomic cores and therefore strongly depends on the coupling to the substrate [28,29].

While at higher energies the dispersions of the two surface states are mostly spatially decoupled, towards the band apex the states are mixed and the net spin polarization decreases. The energy range in which a significant change can be observed is confined close to the band apex. An experimental determination of this reduction (cf. Fig. 2) is intricate as the measured spin polarization amplitude is depending on the measurement geometry, photon energy, and probing depth but in any case it is mostly overshadowed by the larger experimental overlap due to the smaller k separation of the branches.

The main difference between Bi_2Se_3 films and other Rashba systems is that in the latter case the spatial distribution of both spin branches is very similar, whereas here they are localized on different sides of the film [Fig. 3(g)]. This opens the possibility to create a spintronic device where the states on either side of the film can be

manipulated independently of each other. The continuous spatial separation of the surface states upon increasing the film thickness and the accompanying reduction of the gap shows that the topological surface states and their spin polarization do not emerge abruptly at the topological phase transition but develop smoothly from preexisting states. A similar mechanism is discussed in the topological transition of $BiTl(S_{1-x}Se_x)_2$ upon sulfur doping [30,31], where Rashba-like spin-polarized precursor states are observed already on the trivial side of the transition.

In summary, we have performed systematic spin-resolved ARPES measurements on $Bi_2Se_3/InP(111)$ films with thicknesses ranging from 2 to 6 QL. The measurements show that towards lower thicknesses the two surface states hybridize and a gap opens. Because of the substrate-induced structural inversion asymmetry the resultant massive Dirac state is split in a Rashba-like manner with distinct localization of the outer and inner branches at the top and at the bottom boundary of the film, respectively. Our measurements contribute to the understanding of the evolution of the dispersion and the localization of the surface states at the dimensional crossover.

This work was supported by the Swiss National Science Foundation and the EU ERC-AG Program (Project 3-TOP). Part of this work was supported by the Russian Foundation for Basic Research (Grant No. 13-02-12110_ofi_m). G. K. acknowledges funding by the Alexander von Humboldt Foundation.

[1] B. A. Bernevig, T. L. Hughes, and S.-C. Zhang, Science **314**, 1757 (2006).
[2] M. König, S. Wiedmann, C. Brüne, A. Roth, H. Buhmann, L. W. Molenkamp, X.-L. Qi, and S.-C. Zhang, Science **318**, 766 (2007).
[3] L. Fu, C. L. Kane, and E. J. Mele, Phys. Rev. Lett. **98**, 106803 (2007).
[4] D. Hsieh, Y. Xia, D. Qian, L. Wray, J. Dil, F. Meier, J. Osterwalder, L. Patthey, J. Checkelsky, N. Ong, A. Fedorov, H. Lin, A. Bansil, D. Grauer, Y. Hor, R. Cava, and M. Hasan, Nature (London) **460**, 1101 (2009).
[5] M. Z. Hasan and C. L. Kane, Rev. Mod. Phys. **82**, 3045 (2010).
[6] H. Zhang, C.-X. Liu, X.-L. Qi, X. Dai, Z. Fang, and S.-C. Zhang, Nat. Phys. **5**, 438 (2009).
[7] Y. Zhang, K. He, C.-Z. Chang, C.-L. Song, L.-L. Wang, X. Chen, J.-F. Jia, Z. Fang, X. Dai, W.-Y. Shan, S.-Q. Shen, Q. Niu, X.-L. Qi, S.-C. Zhang, X.-C. Ma, and Q.-K. Xue, Nat. Phys. **6**, 584 (2010).
[8] C.-X. Liu, H. J. Zhang, B. Yan, X.-L. Qi, T. Frauenheim, X. Dai, Z. Fang, and S.-C. Zhang, Phys. Rev. B **81**, 041307 (2010).
[9] S. Schreyeck, N. V. Tarakina, G. Karczewski, C. Schumacher, T. Borzenko, C. Brune, H. Buhmann, C. Gould, K. Brunner, and L. W. Molenkamp, Appl. Phys. Lett. **102**, 041914 (2013).
[10] Y. Sakamoto, T. Hirahara, H. Miyazaki, S.-i. Kimura, and S. Hasegawa, Phys. Rev. B **81**, 165432 (2010).
[11] A. Richardella, D. M. Zhang, J. S. Lee, A. Koser, D. W. Rench, A. L. Yeats, B. B. Buckley, D. D. Awschalom, and N. Samarth, Appl. Phys. Lett. **97**, 262104 (2010).
[12] X. F. Kou, L. He, F. X. Xiu, M. R. Lang, Z. M. Liao, Y. Wang, A. V. Fedorov, X. X. Yu, J. S. Tang, G. Huang, X. W. Jiang, J. F. Zhu, J. Zou, and K. L. Wang, Appl. Phys. Lett. **98**, 242102 (2011).
[13] P. Tabor, C. Keenan, S. Urazdhin, and D. Lederman, Appl. Phys. Lett. **99**, 013111 (2011).
[14] S. Muff, F. von Rohr, G. Landolt, B. Slomski, A. Schilling, R. J. Cava, J. Osterwalder, and J. H. Dil, Phys. Rev. B **88**, 035407 (2013).
[15] M. Hoesch, T. Greber, V. N. Petrov, M. Muntwiler, M. Hengsberger, W. Auwaerter, and J. Osterwalder, J. Electron Spectrosc. Relat. Phenom. **124**, 263 (2002).
[16] G. Kresse and J. Hafner, Phys. Rev. B **47**, 558 (1993).
[17] G. Kresse and J. Fürthmuller, Comput. Mater. Sci. **6**, 15 (1996).
[18] J. P. Perdew, K. Burke, and M. Ernzerhof, Phys. Rev. Lett. **77**, 3865 (1996).
[19] P. E. Blöchl, Phys. Rev. B **50**, 17953 (1994).
[20] G. Kresse and D. Joubert, Phys. Rev. B **59**, 1758 (1999).
[21] See Supplemental Material at http://link.aps.org/supplemental/10.1103/PhysRevLett.112.057601 for circular dichroism measurements, SARPES measurements with different photon polarization and energy, and DFT calculations on the spin-orbital texture and thickness dependence.
[22] H. Zhang, C.-X. Liu, and S.-C. Zhang, Phys. Rev. Lett. **111**, 066801 (2013).
[23] Z. H. Zhu, C. N. Veenstra, G. Levy, A. Ubaldini, P. Syers, N. P. Butch, J. Paglione, M. W. Haverkort, I. S. Elfimov, and A. Damascelli, Phys. Rev. Lett. **110**, 216401 (2013).
[24] Y. Cao, J. A. Waugh, X.-W. Zhang, J.-W. Luo, Q. Wang, T. J. Reber, S. K. Mo, Z. Xu, A. Yang, J. Schneeloch, G. D. Gu, M. Brahlek, N. Bansal, S. Oh, A. Zunger, and D. S. Dessau, Nat. Phys. **9**, 499 (2013).
[25] L. Fu, Phys. Rev. Lett. **103**, 266801 (2009).
[26] F. Meier, H. Dil, J. Lobo-Checa, L. Patthey, and J. Osterwalder, Phys. Rev. B **77**, 165431 (2008).
[27] M. Neupane, A. Richardella, J. Sanchez-Barriga, S.-Y. Xu, N. Alidoust, I. Belopolski, C. Liu, G. Bian, D. M. Zhang, D. Marchenko, A. Varykhalov, O. Rader, M. Leandersson, T. Balasubramanian, T.-R. Chang, H.-T. Jeng, S. Basak, H. Lin, A. Bansil, N. Samarth, and M. Z. Hasan, arXiv:1307.5485.
[28] B. Slomski, G. Landolt, F. Meier, L. Patthey, G. Bihlmayer, J. Osterwalder, and J. H. Dil, Phys. Rev. B **84**, 193406 (2011).
[29] A. Varykhalov, J. Sánchez-Barriga, A. M. Shikin, W. Gudat, W. Eberhardt, and O. Rader, Phys. Rev. Lett. **101**, 256601 (2008).
[30] S.-Y. Xu, M. Neupane, C. Liu, S. Jia, L. A. Wray, G. Landolt, B. Slomski, J. H. Dil, N. Alidoust, S. Basak, H. Lin, J. Osterwalder, A. Bansil, R. J. Cava, and M. Z. Hasan, arXiv:1204.6518.
[31] S. Souma, M. Komatsu, M. Nomura, T. Sato, A. Takayama, T. Takahashi, K. Eto, K. Segawa, and Y. Ando, Phys. Rev. Lett. **109**, 186804 (2012).